On the importance of hydrodynamic interactions in polyelectrolyte electrophoresis

2008 J. Phys.: Condens. Matter 20 494217

(http://iopscience.iop.org/0953-8984/20/49/494217)

IOP Publishing Journal of Physics: Condensed Matter

J. Phys.: Condens. Matter **20** (2008) 494217 (6pp) doi:10.1088/0953-8984/20/49/494217

On the importance of hydrodynamic interactions in polyelectrolyte electrophoresis

K Grass[1] **and C Holm**[1,2]

[1] Frankfurt Institute for Advanced Studies, Goethe University, Ruth-Moufang-Strasse 1, D-60438 Frankfurt am Main, Germany
[2] Max-Planck Institute for Polymer Research, Ackermannweg 10, D-55128 Mainz, Germany

E-mail: grass@fias.uni-frankfurt.de and c.holm@fias.uni-frankfurt.de

Received 22 July 2008
Published 12 November 2008
Online at stacks.iop.org/JPhysCM/20/494217

Abstract

The effect of hydrodynamic interactions on the free-solution electrophoresis of polyelectrolytes is investigated with coarse-grained molecular dynamics simulations. By comparing the results to simulations with switched-off hydrodynamic interactions, we demonstrate their importance in modelling the experimentally observed behaviour. In order to quantify the hydrodynamic interactions between the polyelectrolyte and the solution, we present a novel way to estimate its effective charge. We obtain an effective friction that is different from the hydrodynamic friction obtained from diffusion measurements. This effective friction is used to explain the constant electrophoretic mobility for longer chains. To further emphasize the importance of hydrodynamic interactions, we apply the model to end-labelled free-solution electrophoresis.

1. Introduction

Nowadays, electrophoretic separation methods are widely applied to study polyelectrolytes (PEs) such as proteins, DNA and synthetic polymers [1–3]. While there exist several theories [4–7] that have been successfully used to describe qualitatively the experimentally observed behaviour of various PEs, there are still many open problems to address.

Recent experiments on strongly charged flexible PEs, such as polystyrene sulfonate (PSS) and single-stranded DNA (ssDNA) of well-defined length, have shown a characteristic behaviour for the short-chain free-solution mobility μ [8–11]: after an initial increase of the mobility with increasing length, μ passes through a maximum, and then decreases towards a constant mobility for long chains.

The increase for short chains and the long-chain limit can be explained within the theoretical approaches, but the origins of the maximum for intermediate chains remain indistinct. To some extent this can be attributed to the simplifying assumptions made in those models regarding the interplay of the various interactions: the Coulomb interaction between the charged PE monomers and its counterions, the external electric field likewise acting on the charges and the hydrodynamic interactions with the solvent.

To provide a fundamental understanding of the involved dynamics, we believe it is mandatory to study the effects of these forces on a microscopic level, thereby taking into account full electrostatic as well as hydrodynamic interactions. Continuing the work of [12], we use coarse-grained molecular dynamics simulations to determine the transport coefficients and structural properties of strong polyelectrolytes in free-solution electrophoresis. We characterize the hydrodynamic interactions between solvent and solute on a microscopic level, and determine the relevant length scale for these interactions.

This paper is structured as follows: in section 2 we introduce the simulation model and specify all relevant parameters. After comparing the simulation results to experimental measurements of the PSS transport coefficients for varying length (section 3.1), we switch off hydrodynamic interactions to characterize the behaviour in the absence of them. In section 3.4, we introduce the concept for an effective friction of the polyelectrolyte–counterion compound with the surrounding solvent. To quantify the effective friction, we propose a novel way to estimate the effective charge. Finally, we show that the effective friction, measured in this way, deviates from the hydrodynamic friction that can be obtained from diffusion measurements, and that this deviation is the reason for the observable length-independent mobility of long

polyelectrolyte chains. Finally, in section 3.7, we demonstrate how increasing the effective friction by a drag label can restore size-dependent mobility. We finish this paper with concluding remarks.

2. Simulation model

We use a charged bead–spring model within the Espresso package [13] to study the behaviour of flexible linear PEs of different lengths. All parameters are given in reduced units with energy scale $kT = 1.0$ and relevant length scale σ_0 which is used to match the model to a specific polyelectrolyte. For this paper, we chose $\sigma_0 = 2.5$ Å, which is the distance between two charges along a fully sulfonated PSS backbone. The simulation time step is $\tau_0 = 0.01$.

The PE is comprised of N negatively charged monomers carrying a charge of $-1e_0$, where e_0 is the elementary charge.

The monomers are connected by finitely extensible nonlinear elastic (FENE) bonds $U_{\mathrm{FENE}} = \frac{1}{2}kR^2 \ln(1 - (\frac{r}{R})^2)$, with stiffness $k = 30$ and maximum extension $R = 1.5$, and with r being the distance between the interacting monomers [14]. Additionally, a truncated Lennard-Jones or Weeks–Chandler–Anderson (WCA) potential $U_{\mathrm{LJ}} = 4\epsilon((\frac{\sigma}{r})^12 - (\frac{\sigma}{r})^6)$, with depth $\epsilon = 0.25$ and width $\sigma = 1$, is used for excluded-volume interactions [15].

For charge neutrality, N monovalent counterions of charge $+1e_0$ are added that are subject to the same LJ potential. All particles have the same size.

The simulations are carried out under periodic boundary conditions in a rectangular simulation box. The size L of the box is varied to achieve a constant monomer concentration c_{PE} and counterion concentration c_{CI} independent of chain length. To match experimental conditions with a PSS monomer concentration of 1 g 1^{-1} or 5 mM, we vary L between 34 ($N = 2$) and 89 ($N = 32$).

Full electrostatic interactions are calculated with the particle–particle–particle mesh (P3M) algorithm [16]. The Bjerrum length $l_{\mathrm{B}} = e_0^2/4\pi\epsilon kT = 2.84$ in simulation units corresponds to 7.1 Å (the value for water at room temperature).

To account for hydrodynamic interactions (HI), we frictionally couple all particles to a lattice Boltzmann fluid as detailed in [17]. The modelled fluid has a kinematic viscosity $\nu = 3.0$, a fluid density $\rho = 0.864$ and is discretized by a grid with spacing $a = 1.0$. The coupling parameter is $\Gamma_{\mathrm{bare}} = 20.0$.

In order to further characterize the impact of HI on the system's dynamics, we compare it to simulations with a simple Langevin thermostat that does not recover long-range hydrodynamic interactions between the monomers, but only offers local interactions with the solvent. We set the friction parameter $\Gamma_0 = 15.34$ to match the single-particle mobility of the Langevin system to the one with full HI.

2.1. Determining transport coefficients

Using this model, we determine the single-chain diffusion coefficient D and the electrophoretic mobility μ of the model PE from simulations without an applied external field using the following Green–Kubo relations:

$$D = \tfrac{1}{3}\int_0^\infty \langle \vec{v}_c(\tau)\cdot\vec{v}_c(0)\rangle \,\mathrm{d}\tau \tag{1}$$

$$\mu = \frac{1}{3k_{\mathrm{B}}T}\sum_i q_i \int_0^\infty \langle \vec{v}_c(\tau)\cdot\vec{v}_i(0)\rangle \,\mathrm{d}\tau. \tag{2}$$

Here, $\vec{v}_c$ is the centre-of-mass velocity of the PE, $\vec{v}_i$ is the velocity of every charged particle in the system, i.e. monomers of the PE and associated counterions, and q_i is the corresponding charge. The ensemble average ($\langle\cdots\rangle$) is taken over 10^4 statistically independent samples. The integrations use analytic fits for the slowly converging long-time tails.

The advantage of using a Green–Kubo relation (2) for the electrophoretic mobility is that we can obtain both transport coefficients from the same simulation trajectories at zero field. Doing so we avoid conformational changes to the chain structures or the counterion distributions by an artificially high external electric field, which is sometimes used in other simulations to separate the directed electrophoretic motion from the Brownian motion within reasonable computing time. This approach was successfully applied in simulations to determine the electrophoretic mobility of charged colloids [18, 19].

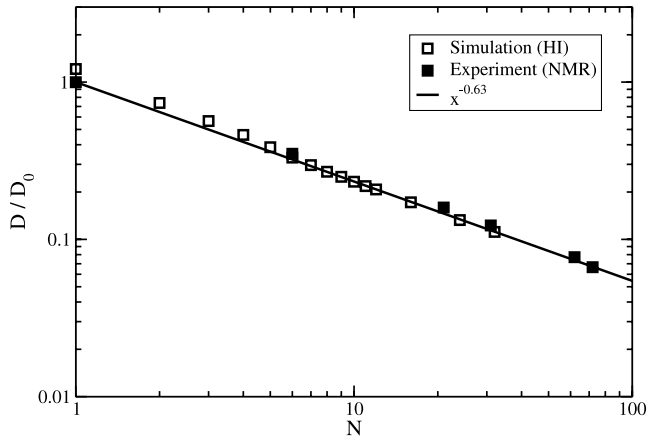

Figure 1. The normalized diffusion coefficient D/D_0 for PSS of different lengths N as obtained by electrophoresis NMR agrees with the simulation results with full hydrodynamic interactions (HI).

3. Results

3.1. Transport coefficients of PSS

In an earlier publication this year [12], we compared the simulation results to experimental data for short PSS obtained by two different experimental methods, namely capillary electrophoresis [8, 20] and pulsed field gradient or electrophoretic NMR [21–24][3].

In figure 1, we compare the diffusion coefficient D determined by simulations to the experimental results. Both

[3] Please refer to [12] for details on the experimental conditions.

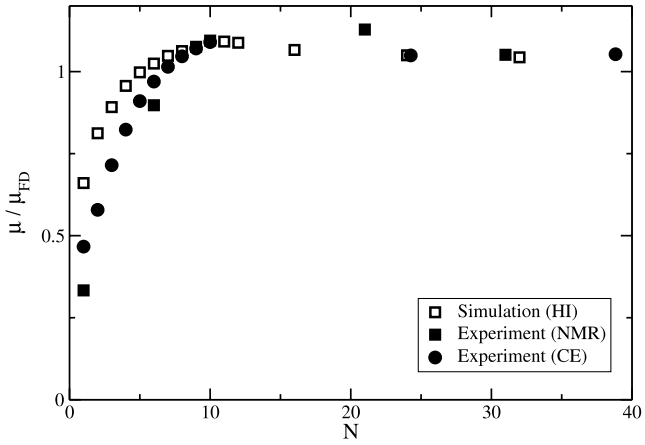

Figure 2. Including hydrodynamic interactions (HI), the normalized electrophoretic mobility μ/μ_{FD} as a function of the number of repeat units N obtained in simulations reproduce a maximum for intermediate chains as well as the long-chain behaviour observed in experiments.

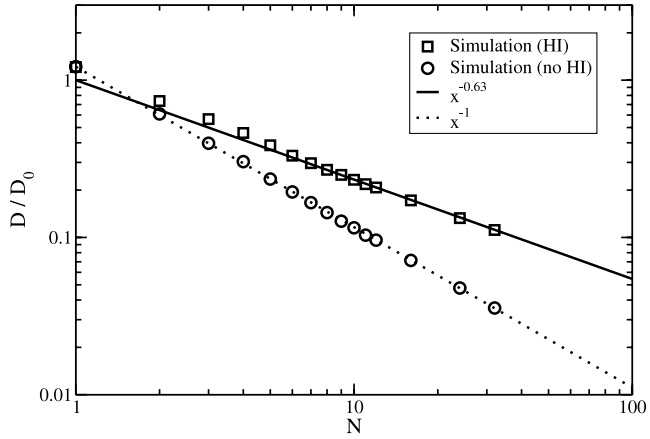

Figure 3. The normalized diffusion coefficient D/D_0 with and without hydrodynamic interactions (HI). With HI the experimentally observed scaling is recovered; without HI the chain diffusion is Rousse-like.

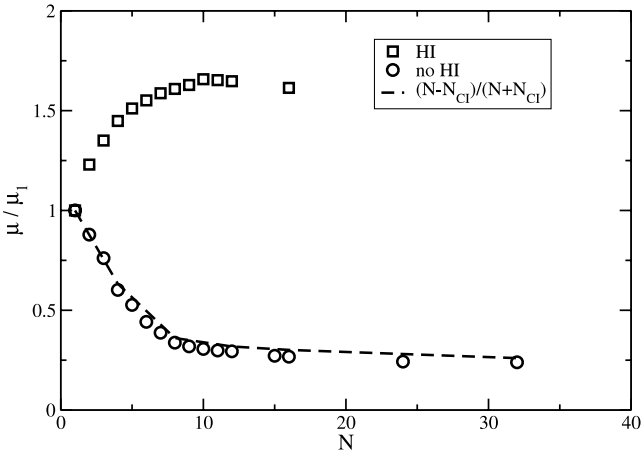

Figure 4. The normalized electrophoretic mobility without hydrodynamic interactions (HI) strongly deviates from the one obtained with HI. The plotted curve, equation (5), describes this observation by using the local force picture.

results are in good agreement and exhibit a power law scaling $D = D_0 N^m$, with an scaling exponent $m = 0.63 \pm 0.01$, which agrees with previous results [11, 25–27]. Here, the simulated data is normalized by $D_0 = 0.052$, the monomer diffusion as obtained by a power law fit, and the experimental data by the monomer diffusion coefficient of $D_0 = 5.7 \times 10^{-10}$ m^2 s^{-1}.

Figure 2 shows the electrophoretic mobility μ normalized by μ_{FD}, the constant (not length-dependent) value for long chains. We compare the simulation results to two different experimental datasets. The simulation results reproduce a maximum for intermediate chains as well as the long-chain behaviour (the constant mobility for long chains) observed in experiments, if the hydrodynamic interactions are properly accounted for.

3.2. Absence of hydrodynamic interactions

Without hydrodynamic interactions, the simulation fails to describe the short-chain behaviour and cannot be mapped to the experimental data.

Figure 3 illustrates the difference in the scaling of the diffusion coefficient with and without hydrodynamic interactions. For the latter, Rousse behaviour is observed with a scaling exponent of $m = 1.02 \pm 0.02$ for the chain diffusion. Likewise, as shown in figure 4, the neglect of hydrodynamic interactions leads to a decreasing electrophoretic mobility for short chains and a constant value for long chains. The same observations were made in a recent publication by Frank and Winkler [28].

3.3. Local force balance

The behaviour in the absence of hydrodynamic interactions can be understood in a local force balance picture. A strongly charged polyelectrolyte such as PSS is surrounded by a cloud of oppositely charged counterions, some of which move with the chain, thus forming a molecular compound with the PE that has a reduced electric charge. This effect is also know as counterion condensation [29]. Without hydrodynamic interactions, every particle of this compound is subject to the same frictional force specified by the Langevin thermostat. For a not too strong applied electric field E, the electrophoretic mobility can be obtained by $\mu = v/E$, where v is the steady-state velocity of the compound (PE and co-moving counterions). The two acting forces, the solvent drag force F_{Solvent} and the electric driving force F_{Field}, are of equal magnitude and opposite direction. We now define N_{CI} to be the number of co-moving counterions. This leads to the following equation for the forces, where $\pm Q$ is the charge of the monomers and the counterions, respectively:

$$F_{\mathrm{Solvent}} = -\Gamma_0 v(N + N_{\mathrm{CI}}) \tag{3}$$

$$F_{\mathrm{Field}} = QE(N - N_{\mathrm{CI}}). \tag{4}$$

From this we can obtain the following expression for the electrophoretic mobility in the absence of hydrodynamic

interactions, where $\mu_0 = 1/\Gamma_0$ is the mobility of a single monomer:

$$\frac{\mu}{\mu_0} = \frac{N - N_{\mathrm{CI}}}{N + N_{\mathrm{CI}}}. \tag{5}$$

For plotting (5) in figure 4, we obtain N_{CI} by counting the average number of counterions found within $2\sigma_0$ of the chain. The local force picture successfully describes the observed behaviour in the absence of hydrodynamic interactions.

In the linear response regime neither the chain structure nor the counterion distribution is affected by the presence of hydrodynamic interactions. Thus, the differences displayed in figures 3 and 4 can only be attributed to different frictional forces with the solvent acting on the PE–counterion compound. In the remainder of this paper, we will investigate this in more detail.

3.4. Introducing hydrodynamic friction

Figure 4 shows that the mobility strongly increases when hydrodynamic interactions are taken into account. In other words, the frictional forces the compound experiences from the solvent are reduced by the hydrodynamic interactions between the monomers and the counterions. The solvent interactions are no longer local, thus (3) and (4) have to be modified:

$$F_{\mathrm{Solvent}} = -\Gamma_{\mathrm{eff}}(N, N_{\mathrm{CI}})v \tag{6}$$

$$F_{\mathrm{Field}} = Q_{\mathrm{eff}}(N, N_{\mathrm{CI}})E. \tag{7}$$

Here, Γ_{eff} and Q_{eff} are the *a priori* unknown effective friction and effective charge of the compound, which depend on the degree of polymerization N of the PE chain as well as on the number of co-moving counterions N_{CI}. Combining both equations leads to a general expression for the electrophoretic mobility:

$$\mu = \frac{Q_{\mathrm{eff}}(N, N_{\mathrm{CI}})}{\Gamma_{\mathrm{eff}}(N, N_{\mathrm{CI}})}. \tag{8}$$

Since the general functional dependence of Γ_{eff} on N and N_{CI} in the presence of hydrodynamic interactions is nontrivial, in all but limiting cases, (8) cannot be used to determine the electrophoretic mobility analytically. However, it can be applied to determine the effective friction from the electrophoretic mobility and the effective charge:

$$\Gamma_{\mathrm{eff}} = Q_{\mathrm{eff}}/\mu. \tag{9}$$

3.5. Estimating the effective charge

As before, the electrophoretic mobility is determined by (2), leaving the task to estimate the effective charge from the simulation. There are several possible ways to determine the number of counterions that shield the bare charge of the polyelectrolyte. In section 3.3, we already used the straightforward way of counting the number of counterions within a tube of radius 2σ around the chain:

$$Q_{\mathrm{eff}}^{(1)} = N - N_{\mathrm{CI}}(d < 2\sigma). \tag{10}$$

This method has the drawback that the threshold, i.e. the size of the tube, is arbitrarily defined. Another frequently used way is the inflection criterion [30, 31], in which the integrated radial counterion distribution is calculated and the inflection point used as a threshold.

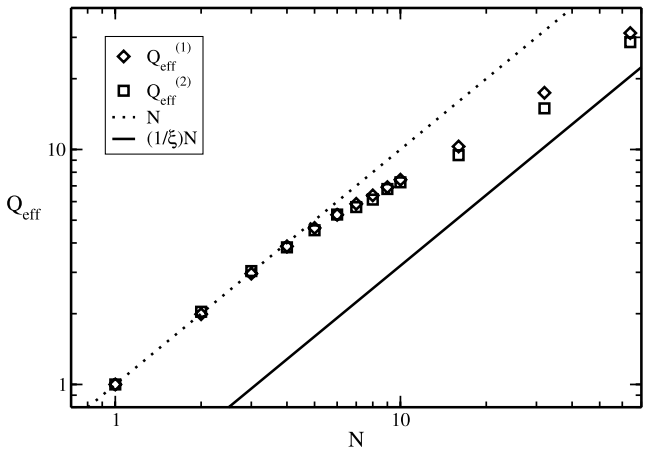

Figure 5. The effective charge Q_{eff} as a function of chain length for both estimators $Q_{\mathrm{eff}}^{(1)}$ and $Q_{\mathrm{eff}}^{(2)}$. The dotted line indicates the bare, unscreened charge of the polyelectrolyte, whereas the full line shows a prediction based on counterion condensation theory, with ξ being the condensation parameter.

Alternatively, we can rewrite (5) and use the electrophoretic mobility without hydrodynamic interactions to calculate the effective charge:

$$Q_{\mathrm{eff}}^{(2)} = N\left(1 - \frac{1 - \mu\Gamma_0}{1 + \mu\Gamma_0}\right). \tag{11}$$

This definition of the effective charge does not have any free parameters and, since simulations without hydrodynamic interactions are computationally inexpensive, we can determine Q_{eff} with high accuracy in this way. Further analysis showed that Q_{eff} is insensitive to hydrodynamic interactions in the linear response regime.

In figure 5, we compare both estimators for the effective charge. For short chains, both estimators agree and coincide with the bare, unscreened charge of the polyelectrolyte. In this regime, no counterion condensation is observed.

For intermediate chains, the effective charge is reduced as it deviates from the bare charge and tends towards the Manning prediction. Here, the condensation parameter for the PSS system is $\xi = 3.12$. In this regime, the simple estimator $Q_{\mathrm{eff}}^{(1)}$ measures a higher effective charge, i.e. not all condensed counterions that are included in the new estimator $Q_{\mathrm{eff}}^{(2)}$ are taken into account.

The so-defined effective charge estimators $Q_{\mathrm{eff}}^{(1)}$ and $Q_{\mathrm{eff}}^{(2)}$ will now be used to quantify the effective friction of the polyelectrolyte–counterion compound.

3.6. Quantifying the effective friction

Figure 6 displays the effective friction of the compound in dependence of the length of the PE chain as obtained from (9) using the estimators $Q_{\mathrm{eff}}^{(1)}$ and $Q_{\mathrm{eff}}^{(2)}$. We compare the obtained result to the effective friction as it can be obtained via the

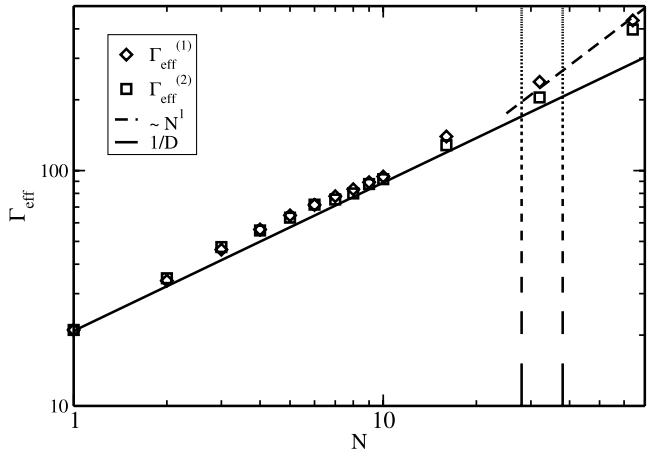

Figure 6. Effective friction of the polyelectrolyte and the co-moving counterions as obtained from (9) using $Q_{\text{eff}}^{(1)}$ and $Q_{\text{eff}}^{(2)}$. For comparison, the inverse diffusion coefficient is displayed, which is a measure of the hydrodynamic friction if the Einstein equation (12) holds. The dashed lines indicate the approximate Debye screening length for the system.

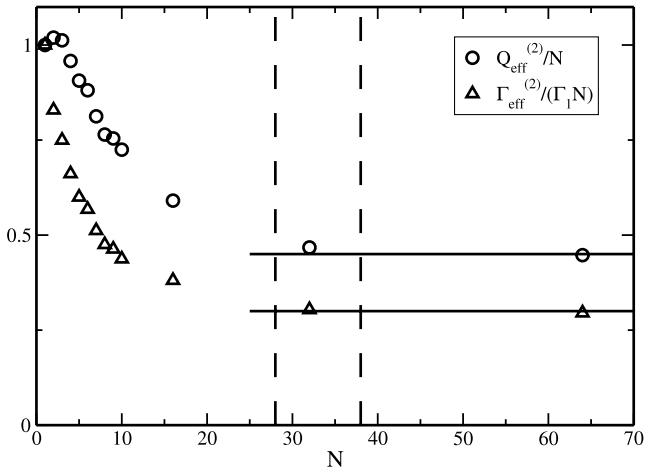

Figure 7. The effective charge and effective friction per monomer as a function of the chain length shows an initially stronger decrease of the friction compared to the charge which leads to the observed increase in mobility. For long chains, both quantities approach a constant value (the lines are visual guides only). Again the dashed lines indicate the range of electrostatic screening.

Einstein equation from measurements of the diffusion of the PE:

$$\Gamma_{\text{D}} = \frac{1}{D}. \tag{12}$$

For chains with contour lengths of the order of the Debye length, a clear deviation between Γ_{eff} and Γ_{D} is observed. Beyond this length scale, the effective friction of the PE increases almost linearly with chain length, whereas the inverse diffusion scales with an exponent of $m = 0.63$, as shown in section 3.1.

In figure 7, we compare the effective friction and the effective charge per monomer. First, the effective friction shows a stronger decrease than the effective charge. This leads to the observed increase in mobility (see figure 4). For longer chains, both quantities approach a constant value. Again the relevant length scale seems to be the Debye length, beyond which both quantities become constant (i.e. linear scaling of Q_{eff} and Γ_{eff}).

This gives us a microscopic understanding of the effects, that lead to the experimentally observed length-independent mobility of long flexible polyelectrolytes. The hydrodynamic interactions between polyelectrolyte and counterions decrease the effective friction of the compound on length scales smaller than the electrostatic screening length. For compounds of longer chains, the hydrodynamic interactions are screened and the friction increases linearly with the size of the PE.

As an application of the presented model, we will now look at the possible way to increase the effective friction of the compound.

3.7. Increasing the effective friction

As suggested by Mayer *et al* [32, 33] attaching a drag label ('molecular parachute') to one end of the PE increases the hydrodynamic friction by a constant amount independent of the chain length. This leads to a changed scaling behaviour of the effective friction, which in turn can be seen in a restoration of the size-dependent mobility even for long PE chains.

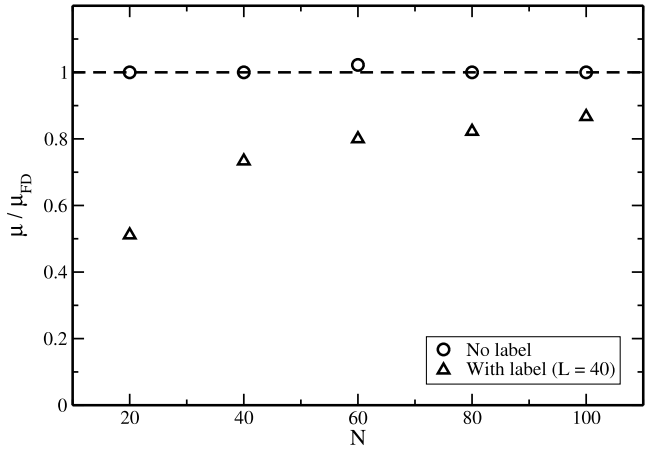

Figure 8. The mobility of a long flexible polyelectrolyte without a label is independent of the chain length N (the line is a visual guide only). With a label of $L = 40$ uncharged beads attached to the polyelectrolyte, the size dependence of the electrophoretic mobility can be recovered.

In the simulations, the label consists of $L = 40$ uncharged monomers attached to one end of the PE chain. The hydrodynamic interactions with the fluid cause an additional force acting on the PE. Figure 8 demonstrates the effectiveness of this method.

In the future, we will use the toolkit described in this paper to analyse the ELFSE process in more detail.

4. Conclusions

We used a coarse-grained MD model to describe unlabelled and labelled free-solution electrophoresis of flexible polyelectrolytes. The simulation results are in good quantitative agreement with experimental data. We used simulations without

hydrodynamic interactions to efficiently measure the effective charge of the polyelectrolyte as a function of the chain length. In a further step, we quantified the effective friction of the compound formed by the polyelectrolyte and co-moving counterions. Our results show that, on a length scale that is of the order of the Debye length for electrostatic screening, the friction becomes linear in terms of the chain length. This increase in friction is exactly cancelled out by the likewise linearly increasing effective charge, leading to the well-known constant mobility for long flexible polyelectrolyte chains.

Acknowledgments

We thank B Dünweg, U Schiller and G Slater for helpful remarks. Funds from the Volkswagen Foundation, the DAAD and DFG under grant no. TR6 are gratefully acknowledged.

References

[1] Righetti P G (ed) 1996 *Capillary Electrophoresis in Analytical Biotechnology* (Boca Raton, FL: CRC Press)
[2] Cottet H, Simo C, Vayaboury W and Cifuentes A 2005 Nonaqueous and aqueous capillary electrophoresis of synthetic polymers *J. Chromatogr.* A **1068** 59–73
[3] Dolnik V 2006 Capillary electrophoresis of proteins 2003–2005 *Electrophoresis* **27** 126–41
[4] Barrat J-L and Joanny J-F 1996 Theory of polyelectrolyte solutions *Adv. Chem. Phys.* **94** 1–66
[5] Muthukumar M 1996 Theory of electrophoretic mobility of a polyelectrolyte in semidilute solutions of neutral polymers *Electrophoresis* **17** 1167–72
[6] Volkel A R and Noolandi J 1995 On the mobility of stiff polyelectrolytes *J. Chem. Phys.* **102** 5506–11
[7] Mohanty U and Stellwagen N C 1999 Free solution mobility of oligomeric DNA *Biopolymers* **49** 209–14
[8] Stellwagen E and Stellwagen N C 2002 Determining the electrophoretic mobility and translational diffusion coefficients of DNA molecules in free solution *Electrophoresis* **23** 2794–803
[9] Hoagland D A, Arvanitidou E and Welch C 1999 Capillary electrophoresis measurements of the free solution mobility for several model polyelectrolyte systems *Macromolecules* **32** 6180–90
[10] Cottet H, Gareil P, Theodoly O and Williams C E 2000 A semi-empirical approach to the modeling of the electrophoretic mobility in free solution: application to polystyrenesulfonates of various sulfonation rates *Electrophoresis* **21** 3529–40
[11] Stellwagen E, Lu Y J and Stellwagen N C 2003 Unified description of electrophoresis and diffusion for DNA and other polyions *Biochemistry* **42** 11745–50
[12] Grass K, Böhme U, Scheler U, Cottet H and Holm C 2008 Importance of hydrodynamic shielding for the dynamic behavior of short polyelectrolyte chains *Phys. Rev. Lett.* **100** 096104
[13] Limbach H J, Arnold A, Mann B A and Holm C 2006 ESPResSo—an extensible simulation package for research on soft matter systems *Comput. Phys. Commun.* **174** 704–27
[14] Soddemann T, Dünweg B and Kremer K 2001 A generic computer model for amphiphilic systems *Eur. Phys. J.* E **6** 409
[15] Weeks J D, Chandler D and Andersen H C 1971 Role of repulsive forces in determining the equilibrium structure of simple liquids *J. Chem. Phys.* **54** 5237
[16] Deserno M and Holm C 1998 How to mesh up Ewald sums. I. A theoretical and numerical comparison of various particle mesh routines *J. Chem. Phys.* **109** 7678
[17] Ahlrichs P and Dünweg B 1999 Simulation of a single polymer chain in solution by combining lattice boltzmann and molecular dynamics *J. Chem. Phys.* **111** 8225–39
[18] Lobaskin V, Dünweg B, Medebach M, Palberg T and Holm C 2007 Electrophoresis of colloidal dispersions in the low-salt regime *Phys. Rev. Lett.* **98** 176105
[19] Dünweg B, Lobaskin V, Seethalakshmy-Hariharan K and Holm C 2008 Colloidal electrophoresis: scaling analysis, Green–Kubo relation, and numerical results *J. Phys.: Condens. Matter* **20** 404214
[20] Nkodo A E, Garnier J M, Tinland B, Ren H, Desruisseaux C, McCormick L C, Drouin G and Slater G W 2001 Diffusion coefficient of DNA molecules during free solution electrophoresis *Electrophoresis* **22** 2424–32
[21] Stejskal E O and Tanner J E 1965 Spin diffusion measurements-spin echoes in presence of a time-dependent field gradient *J. Chem. Phys.* **42** 288
[22] Scheler U 2002 *Handbook of Polyelectrolytes and Their Application* vol 2, ed S K Tripaty, J Kumar and H S Nalwa (Los Angeles, CA: American Scientific) p 173ff
[23] Gottwald A, Kuran P and Scheler U 2003 Separation of velocity distribution and diffusion using PFG NMR *J. Magn. Reson.* **162** 364–70
[24] Stilbs P and Furo I 2006 Electrophoretic NMR *Curr. Opinion Colloid Interface Sci.* **11** 3–6
[25] Böhme U and Scheler U 2003 Effective charge of poly(styrenesulfonate) and ionic strengthen electrophoresis NMR investigation *Colloids Surf.* A **222** 35–40
[26] Böhme U and Scheler U 2007 Effective charge of polyelectrolytes as a function of the dielectric constant of a solution *J. Colloid Interface Sci.* **309** 231–5
[27] Böhme U and Scheler U 2007 Hydrodynamic size and electrophoretic mobility of poly(styrene sulfonate) versus molecular weight *Macromol. Chem. Phys.* **208** 2254–7
[28] Frank S and Winkler R G 2008 Polyelectrolyte electrophoresis: field effects and hydrodynamic interactions *Europhys. Lett.* **83** 38004
[29] Manning G S and Ray J 1998 Counterion condensation revisited *J. Biomol. Struct. Dyn.* **16** 461–76
[30] Belloni L, Drifford M and Turq P 1984 Counterion diffusion in polyelectrolyte solutions *Chem. Phys.* **83** 147
[31] Deserno M, Holm C and May S 2000 The fraction of condensed counterions around a charged rod: comparison of Poisson–Boltzmann theory and computer simulations *Macromolecules* **33** 199–206
[32] Mayer P, Slater G W and Drouin G 1994 Theory of DNA-sequencing using free-solution electrophoresis of protein–DNA complexes *Anal. Chem.* **66** 1777–80
[33] Heller C, Slater G W, Mayer P, Dovichi N, Pinto D, Viovy J L and Drouin G 1998 Free-solution electrophoresis of DNA *J. Chromatogr.* A **806** 113–21